Hindawi Publishing Corporation
Journal of Biomedicine and Biotechnology
Volume 2012, Article ID 672428, 9 pages
doi:10.1155/2012/672428

Research Article

Alterations in Cell Cycle and Induction of Apoptotic Cell Death in Breast Cancer Cells Treated with α-Mangostin Extracted from Mangosteen Pericarp

Hitomi Kurose,[1] Masa-Aki Shibata,[2] Munekazu Iinuma,[3] and Yoshinori Otsuki[1]

[1] *Division of Life Sciences, Department of Anatomy and Cell Biology, Osaka Medical College, 2-7 Daigaku-machi, Takatsuki, Osaka 569-8686, Japan*
[2] *Laboratory of Anatomy and Histopathology, Faculty of Health Science, Osaka Health Science University, 1-9-27 Temma, Kita-ku, Osaka 530-0043, Japan*
[3] *Laboratory of Pharmacognosy, Faculty of Pharmacy, Gifu Pharmaceutical University, 1-25-4 Daigaku-nishi, Gifu 501-1196, Japan*

Correspondence should be addressed to Yoshinori Otsuki, an1001@art.osaka-med.ac.jp

Received 31 July 2011; Revised 2 November 2011; Accepted 20 November 2011

Academic Editor: Ikhlas A. Khan

The development of molecularly targeted drugs has greatly advanced cancer therapy, despite these drugs being associated with some serious problems. Recently, increasing attention has been paid to the anticancer effects of natural products. α-Mangostin, a xanthone isolated from the pericarp of mangosteen fruit, has been shown to induce apoptosis in various cancer cell lines and to exhibit antitumor activity in a mouse mammary cancer model. In this study, we investigated the influence of α-mangostin on apoptosis and cell cycle in the human breast cancer cell line MDA-MB231 (carrying a p53 mutation, and HER2, ER, and PgR negative) in order to elucidate its anticancer mechanisms. In α-mangostin-treated cells, induction of mitochondria-mediated apoptosis was observed. On cell-cycle analysis, G1-phase arrest, increased $p21^{cip1}$ expression and decreases in cyclins, cdc(s), CDKs and PCNA were observed. In conclusion, α-mangostin may be useful as a therapeutic agent for breast cancer carrying a p53 mutation and having HER2- and hormone receptor-negative subtypes.

1. Introduction

Various molecularly targeted drugs against a range of cancers, including breast cancer, have recently been developed. Trastuzumab is a monoclonal antibody against human epidermal growth factor (HER/ErbB) receptor 2 (HER2/ErbB2). Around 15–20% of patients with breast cancer have HER2-positive tumors, and overexpression of HER2 is observed in these patients [1]. Trastuzumab has been shown to induce tumor regression in such patients. Sunitinib, sorafenib, and bevacizumab are multitargeted tyrosine kinase inhibitors that inhibit tumor neovascularization and are currently in clinical trials [2, 3]. These drugs are associated with serious problems such as adverse effects, drug resistance, and low efficacy of single therapy, particularly against metastatic or recurrent breast cancer. Hormone therapy has also been used against hormone receptor-positive breast cancer. However, about 10 to 15% of breast cancers do not express either estrogen or progesterone receptor (ER and PgR, resp.) and do not overexpress the HER2 gene [4].

Mangosteen (*Garcinia mangostana* Linn) pericarp contains various phytochemicals, primarily xanthones, and the resin extracts have long been used for medicinal purposes in Southeast Asia [5]. α-Mangostin is a one of xanthones present in mangosteen pericarp (78% content). A recent study has shown that α-mangostin induces cell-cycle arrest and apoptosis in various types of human cancer cells [5–8]. We previously reported that α-mangostin significantly inhibits both tumor growth and metastasis in a mouse model of mammary cancer [9, 10]. In addition, α-mangostin treatment significantly decreased the levels of phospho-Akt-threonine 308(Thr308) in a human mammary carcinoma cell line and mammary carcinoma tissues *in vivo* [10].

Here, we investigated the antitumor potential of α-mangostin on apoptosis and cell cycle arrest in a human breast cancer cell line carrying a p53 mutation and having HER2-, ER-, and PgR-negative status.

2. Materials and Methods

2.1. Experimental Regimen. Mangosteen (*Garcinia mangostana* Linn) pericarps were dried, ground, and successively extracted in water and 50% ethanol. After freeze-drying the 50% ethanol extract, the resultant dried powder was suspended in water partitioned with ethyl acetate. The ethyl acetate extract was then purified by chromatography on silica gel with the n-hexane-ethyl acetate system and recrystallized to give α-mangostin at >98% purity. For *in vitro* use, crystallized α-mangostin was dissolved in dimethyl sulphoxide (DMSO), and aliquots of stock 20 mM solution were stored at −20°C.

2.2. Cell Line. The MDA-MB231, a human mammary carcinoma cell line stably expressing the green fluorescence protein (GFP) [11], was maintained in RPMI-1640 medium containing 10% fetal bovine serum with streptomycin/penicillin in an incubator under 5% CO_2. MDA-MB231 cells have a p53 mutation [12, 13] and HER2-, ER-, and PgR, negative feature [14].

2.3. Cell Viability. MDA-MB231 cells were grown in RPMI-1640 medium supplemented with 10% bovine serum under an atmosphere of 95% air and 5% CO_2 at 37°C. These cells were plated into 96-well plates (1×10^4 cells/well) one day before α-mangostin treatment. They were subsequently incubated for 24 h with culture medium containing DMSO vehicle alone (control) or with medium containing α-mangostin at various concentrations up to 48 μM. Cell viability was determined using a Cell-Titer-Bule Cell Viability Assay (Promega Co., Madison, WI, USA). The IC_{50} under these conditions was found to be 20 μM α-mangostin for 24 h treated and 16 μM for 48 h treated in MDA-MB231 cells; thus, all *in vitro* studies were performed using 20 μM α-mangostin.

2.4. Time-Lapse Imaging. Cells were grown on 35 mm culture dishes under the above-mentioned condition. These cells were subsequently incubated for 24 h with culture medium containing DMSO vehicle alone (control) or with medium containing 20 μM α-mangostin. Imaging has started when the reagents were added into dishes. Time-lapse images were taken using the fluorescence microscope BZ8000 (Keyence, Osaka, Japan).

2.5. Nuclear Staining. For nuclear staining, DAPI with mounting medium (Vector Laboratories, Inc., Burlingame, CA, USA) was used after immunofluorescence staining. For morphological examination of apoptotic changes, Hoechst33342 (Lonza Walkersville, Inc., Walkersville, MD, USA) was added to cultured medium at a concentration of 5 μg/mL.

2.6. Caspase Activity. MDA-MB231 cells were plated into 96-well plates at a concentration of 1×10^4 cells/well one day before α-mangostin treatment. Cells were treated with 20 μM α-mangostin or DMSO alone for 24 h. The activities of caspase-3, caspase-8, caspase-9, and caspase-4 were measured using a Fluorometric Protease Assay Kit (MBL, Inc., Nagoya, Japan) in which cells were lysed with Cell Lysis Buffer contained in this kit and the protein concentration adjusted to 50 μg in each sample. Caspase activity was measured in terms of fluorescence intensity produced by caspase cleavage of the corresponding substrate, using Fluoroskan Ascent (Thermo Election Co., Helsinki, Finland).

2.7. Cell-Cycle Distribution. Flow cytometric analysis was conducted on trypsinized MDA-MB231 cell suspensions that were harvested after a 24 h treatment with 20 μM α-mangostin and fixed in cold 70% ethanol. The cells were stained with a 50 μg/mL propidium iodide solution containing 100 μg/mL RNase A for 20 min at 37°C and then placed on ice just prior to flow cytometric analysis (EPICS Elite ESP; Coulter Co., Miami, FL, USA). The percentage of cells in each phase of the cell cycle was determined using a Multicycle Cell-Cycle Analysis program (Coulter Co.).

2.8. ssDNA Analysis. MDA-MB231 cells were plated into 96-well plates at a concentration of 1×10^4 cells/well one day before α-mangostin treatment. Cells were treated with 20 μM α-mangostin or DMSO alone for 24 h. Single-Strand break DNA (ssDNA) levels were detected by using ApoStrand ELISA Apoptosis Detection Kit (Enzo Life Sciences International, Inc., Butler Pike Plymouth Meeting, PA, USA) and measured using Microplate reader (Corona ELECTRIC Co. Ltd., Ibaraki, Japan).

2.9. Cytochrome c Release. Cytochrome *c* leaving the mitochondrial membrane was measured using the InnoCyte Flow Cytometric Cytochrome *c* Release Kit (Merck; Darmstadt, Germany). MDA-MB231 cells were harvested after a 24 h treatment with 20 μM α-mangostin or DMSO alone and 1×10^6 cells were resuspended in 300 μL Permeabilization Buffer to remove the cytosolic cytochrome *c*. The cells were fixed 4% paraformaldehyde and washed. After treatment with blocking buffer, the cells were treated with anticytochrome *c* mouse monoclonal antibody (clone 7H8, Santa Cruz, Biotechnology, CA, USA), followed by secondary antibody conjugated to FITC. Then, the cells were analyzed using a flow cytometer, BD FACSAria (Becton Dickinson, Franklin Lakes, NJ, USA).

2.10. Immunofluorescence Staining. MDA-MB231 cells were grown on 24 mm × 24 mm cover glasses and fixed in 4% formaldehyde solution in phosphate buffer. Immunofluorescence staining was performed with anti-PCNA mouse monoclonal antibody (clone PC10; Cell Signaling Technology, Danvers, MA, USA), cyclin D1 rabbit monoclonal antibody (clone 92G2; Cell Signaling Technology), $p21^{cip1}$ rabbit polyclonal antibody (clone C-19; Santa Cruz Biotechnology). These antibodies were also used in Western blotting.

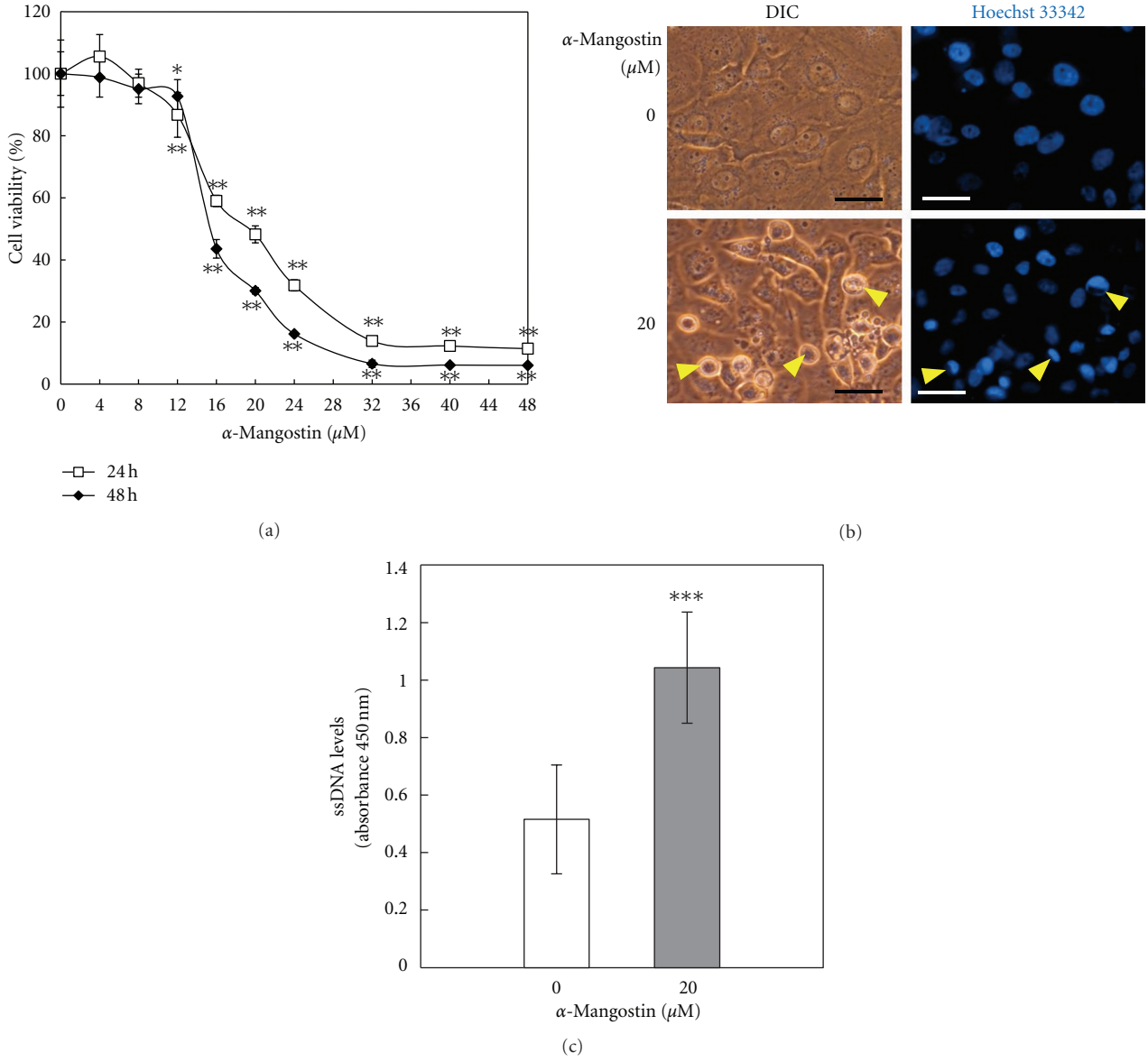

Figure 1: Cell viability and apoptosis detection in MDA-MB231 cells after α-mangostin treatment. (a) Cell viability was significantly lower in human mammary carcinoma MDA-MB231 cells treated with more than 12 μM α-mangostin for 24 or 48 h (*$P < 0.05$, **$P < 0.01$). Five samples from each of α-mangostin dosage were examined. The IC_{50} concentration was determined to be 20 μM for 24 h; therefore, 20 μM α-mangostin was used for all *in vitro* studies. (b) Morphological changes in MDA-MB231 cells treated with 20 μM α-mangostin for 24 h, as compared to controls. Upper two panels show controls and lower two panels show α-mangostin-treated cells. α-Mangostin-treated cells appeared shrunken and chromatin condensation was observed (yellow arrow heads in lower right panel). Scale bars = 50 μm. (c) ssDNA levels were determined by ELISA and were significantly elevated in cells treated with α-mangostin for 24 h, as compared to control levels (***$P < 0.001$). Data are presented as mean ± SD. For all analyses, five samples from control and α-mangostin-treated cells were examined.

2.11. Western Blotting. Total protein was extracted from whole cell lysates of MDA-MB231 cells treated with DMSO or α-mangostin according to the IC_{50} data previously stated. Total protein (40 μg) was fractionated on 16% SDS-PAGE mini gels (TEFCO, Tokyo, Japan) under reducing conditions and transferred to PVDF membranes (Immobilon - P Transfer Membrane, Millipore; Billerica, MA, USA). The membranes were activated in 100% methanol for 15 seconds and incubated with primary antibodies for the following proteins: cytochrome *c*, Bid, PCNA, cyclin D1, $p21^{cip1}$, and β-actin. Membranes were then incubated with the corresponding secondary antibodies conjugated with horseradish peroxidase (HRP). β-Actin (clone N-21) and Full-length Bid (clone FL-195) antibodies were from Santa Cruz Biotechnology. Antibody recognizing cleaved Bid was obtained from R&D Systems (R&D Systems, Inc, Minneapolis, MN, USA). Antibody binding was subsequently visualized by exposure to an enhancing chemiluminescence reagent (Amersham ECL;

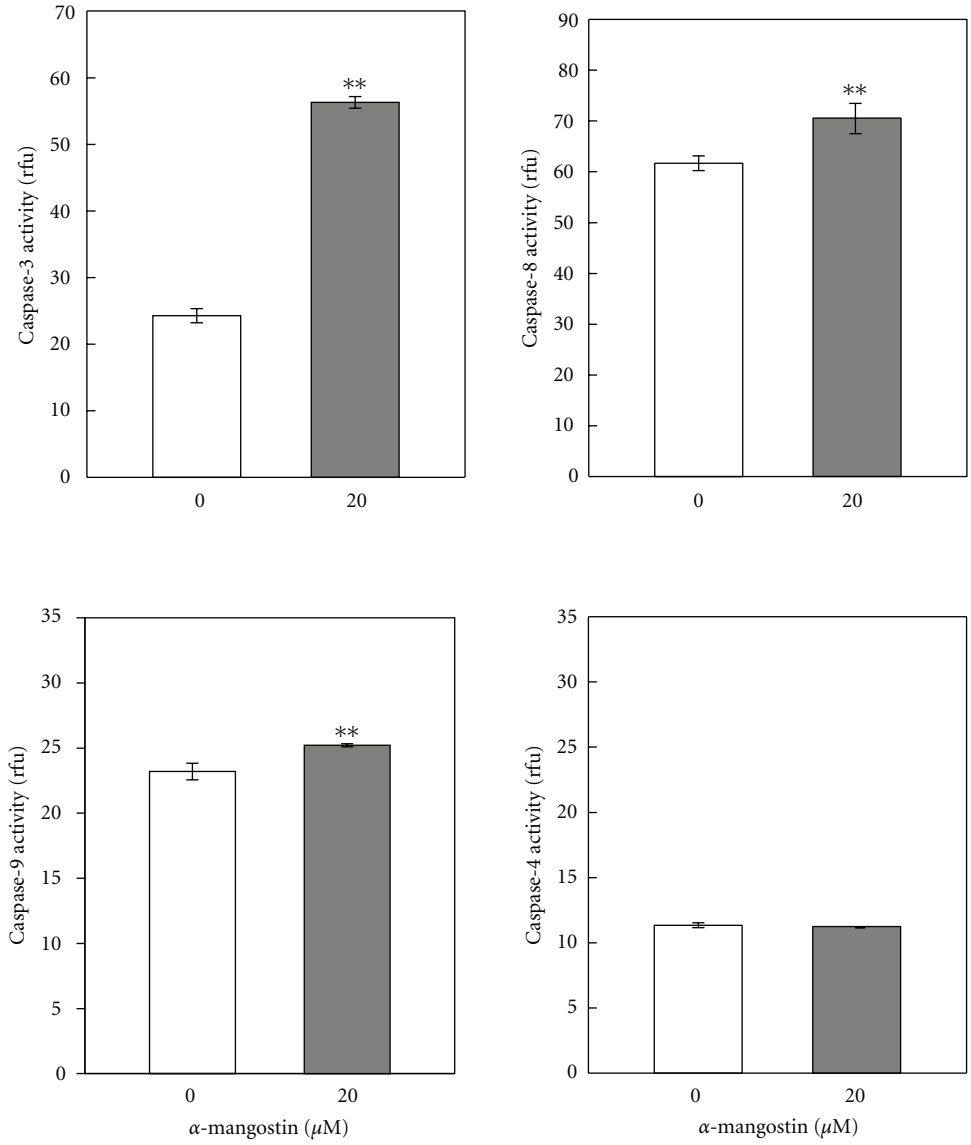

Figure 2: Caspase activity of MDA-MB231 cells after treatment with α-mangostin. Caspase activity was evaluated by luminescence assay. Activity of caspase-3, caspase-8, and caspase-9, but not caspase-4, was significantly elevated in MDA-MB231 cells treated with 20 μM α-mangostin for 24 h (**$P < 0.01$). Data are presented as mean ± SD. Five samples from control and α -mangostin-treated cells were used for measurement of caspase activity.

GE Healthcare UK Ltd., Buckinghamshire, UK). Blots were visualized using a LAS-3000 image analyzer (Fujifilm, Co., Tokyo, Japan).

2.12. Real-Time PCR. MDA-MB231 cells were treated with DMSO or 20 μM α-mangostin for 6, 12, and 24 h. Protein was extracted using cell lysis buffer containing protease and phosphatase inhibitor cocktail. Total RNA was extracted from these cells with FastPure RNA kit (Takara Bio Inc., Shiga, Japan) and cDNAs were synthesized with PrimeScript RT reagent kit (Takara Bio Inc.). Primers involved in the cell-cycle regulation were used containing PrimerArray Cell cycle (human) (Takara Bio Inc.) and real-time PCR reaction was performed with Thermal Cycler Dice Real Time (Takara Bio Inc.). Data were corrected against glyceraldehyde-3-phosphate dehydrogenase (GAPDH) values and expressed as mean ± SD.

2.13. Statistical Analysis. Significant differences in the quantitative data between groups were analyzed using Student's *t*-test via the method of Welch, and *P* values less than 0.05 were considered to represent a statistically significant difference.

3. Results and Discussion

3.1. Cell Viability. Viability analyses of MDA-MB231 human mammary cancer cells showed significantly lower viability

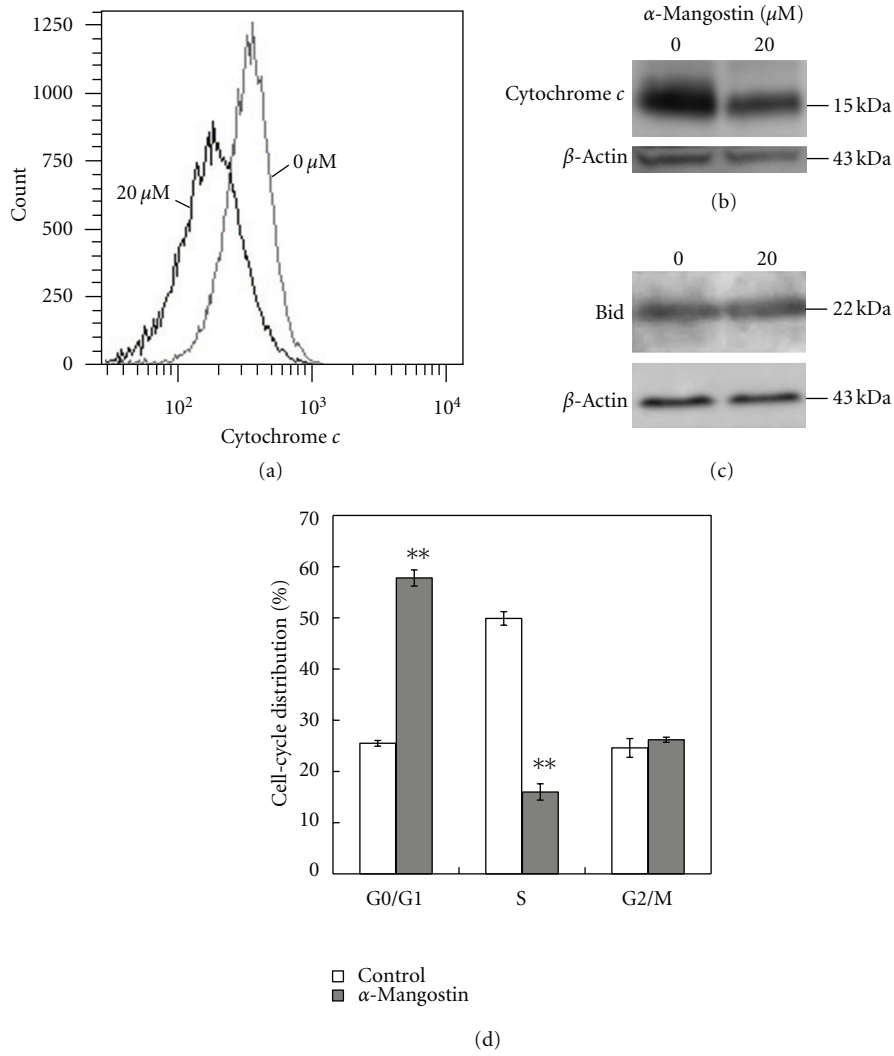

Figure 3: Cytochrome *c* expression, Bid cleavage, and cell-cycle distribution of MDA-MB231 cells after α-mangostin treatment. (a) Cytochrome *c* in mitochondria, as determined by flow cytometry (black line indicates α-mangostin-treated cells and gray line indicates controls). The levels of cytochrome *c* protein in mitochondrial fractions were significantly lower in cells treated with α-mangostin for 24 h (b). Western blots of cytochrome *c* (15 kDa) showed significant decreases in cells treated with α-mangostin for 24 h, as compared to controls (upper panel). In α-mangostin-treated cells, cytochrome *c* was released from mitochondria, leading to decreases in concentration. β-Actin served as an internal control (lower panel, same in (c)). (c) Western blots of Bid (22 kDa) in control cells and cells treated with α-mangostin for 24 h were similar (upper panel). Cleaved Bid was not observed after α-mangostin treatment. Three samples were used for all analyses in (a)–(c). (d) Cell-cycle analysis confirmed that α-mangostin induced arrest in the G1-phase and inhibition of cells entering the S-phase in MDA-MB231 cells ($^{**}P < 0.01$). Data are presented as mean ± SD of triplicate, independent measurements.

after 24 and 48 h of treatment with more than 12 μM α-mangostin (Figure 1(a)). Based on the IC_{50} data, 20 μM was determined to be the optimal concentration of α-mangostin for *in vitro* studies.

3.2. Morphological Changes. For morphological examination of apoptotic changes, MDA-MB231 cells were stained with Hoechst 33342 (Figure 1(b)). After 20 μM α-mangostin treatment for 24 h, cells appeared shrunken and chromatin condensation was observed (yellow arrow heads in lower right panel). These changes suggest that the antiproliferative effects of α-mangostin are associated with apoptosis in MDA-MB231 human mammary cancer cells. Furthermore, we performed time-lapse imaging from the start of 20 μM α-mangostin treatment for 24 h. After 6 h, cell proliferation started to decrease significantly and cell shape had changed after 12 h (data not shown).

3.3. Apoptosis Studies

3.3.1. ssDNA Analysis. In order to confirm that the morphological changes observed after α-mangostin treatment occurred as a consequence of apoptosis, we measured ssDNA levels of α-mangostin treated cells, as compared to controls. In α-mangostin-treated cells, ssDNA levels were significantly elevated ($P < 0.001$, Figure 1(c)). This suggests that the

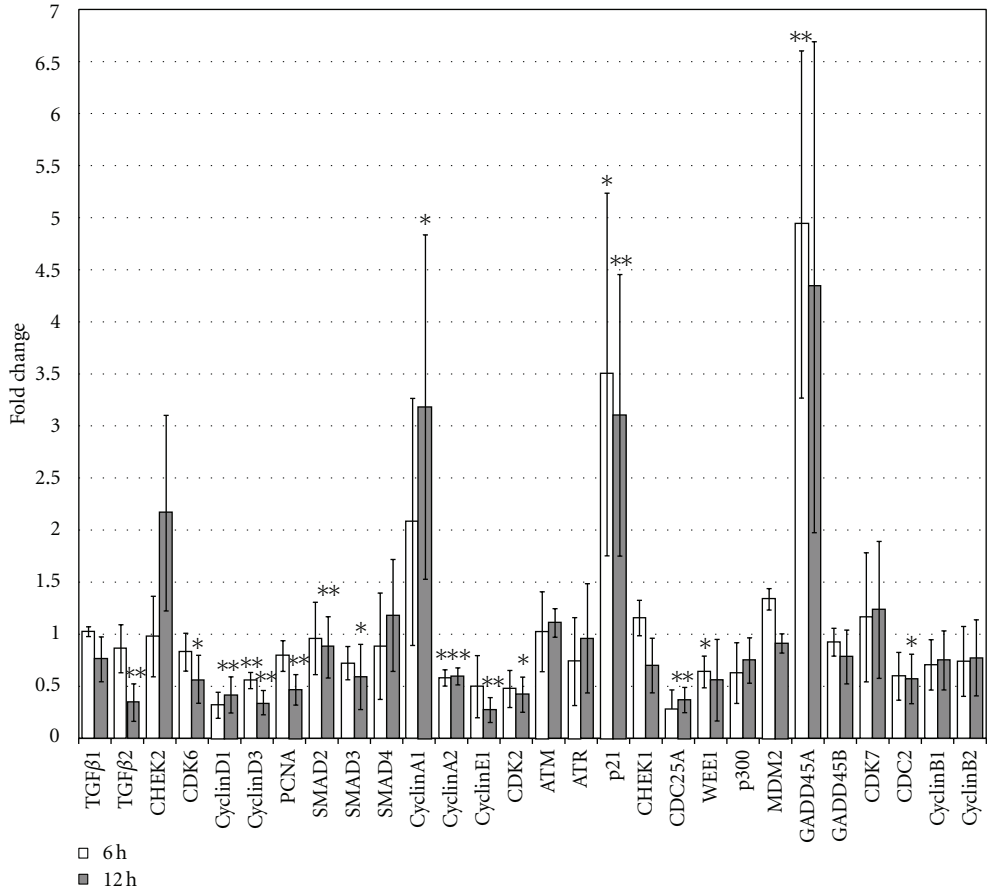

Figure 4: Real-time PCR analysis of gene expression associated with cell cycle. mRNA expression of cell-cycle-related genes, such as cyclins, cdc(s), CDKs, and PCNA, was examined by real-time PCR assay in MDA-MB231 cells after treatment with α-mangostin, as compared with controls. White bars and gray bars show the results of analysis for 6 h and 12 h after treatment with 20 μM α-mangostin, respectively ($^*P < 0.05$, $^{**}P < 0.01$). Relative levels of target gene expression were calculated using the $\Delta\Delta$ CT method. GAPDH was used as a reference gene. Data are presented as means $\pm$ SD of triplicate independent measurements.

morphological changes in human mammary cancer cells that occurred after α-mangostin treatment were caused by apoptosis.

3.3.2. Caspase Activity. Significantly elevated caspase-3, caspase-8, and caspase-9 activity was observed in MDA-MB231 cells treated with α-mangostin for 24 h (Figure 2), as compared to controls. The activity of caspase-4 did not differ significantly between control cells and α-mangostin-treated cells (Figure 2). These results indicate that α-mangostin-induced mitochondria mediated apoptosis.

3.3.3. Cytochrome c Release. In order to confirm mitochondria-mediated apoptosis, levels of cytochrome *c* were measured by flow cytometry and Western blot. The levels of cytochrome *c* protein in mitochondrial fractions were significantly lower in cells treated with α-mangostin for 24 h (Figure 3(a)). Cytochrome *c* protein was released from mitochondria, leading to decreases in concentration (Figure 3(b)). These results were strongly suggesting engagement of the mitochondria-mediated apoptotic pathway.

3.3.4. Bid Cleavage. As caspase-8 activity was elevated, we examined whether the mitochondrial pathway was activated via caspase-8-Bid cleavage by performing Western blots for Bid. Full-length Bid (22 kDa) was equally detected in control cells and in cells treated with α-mangostin for 24 h (Figure 3(c)); this indicates that no Bid cleavage occurred. In addition, no cleaved Bid (15 kDa) was observed when using cleaved Bid-detectable antibody in any of the groups (data not shown). These results suggest that apoptosis was induced by α-mangostin via mitochondria, but was not accompanied by Bid cleavage. We previously reported that α-mangostin decreased phospho-Akt-Th308 in MDA-MB231 cells and mammary carcinoma tissues [10]. Akt is a serine/threonine protein kinase that mediates the downstream effects of phosphatidylinositol 3-kinase (PI3K) by phosphorylating multiple targets involved in regulating diverse cellular functions, including proliferation, growth, and survival. Therefore, Akt phosphorylation by therapeutic agents leads to growth inhibition, cell-cycle arrest, and apoptosis in cancer cells. A previous study in human colon cancer cells showed that α-mangostin inhibited Erk1/2

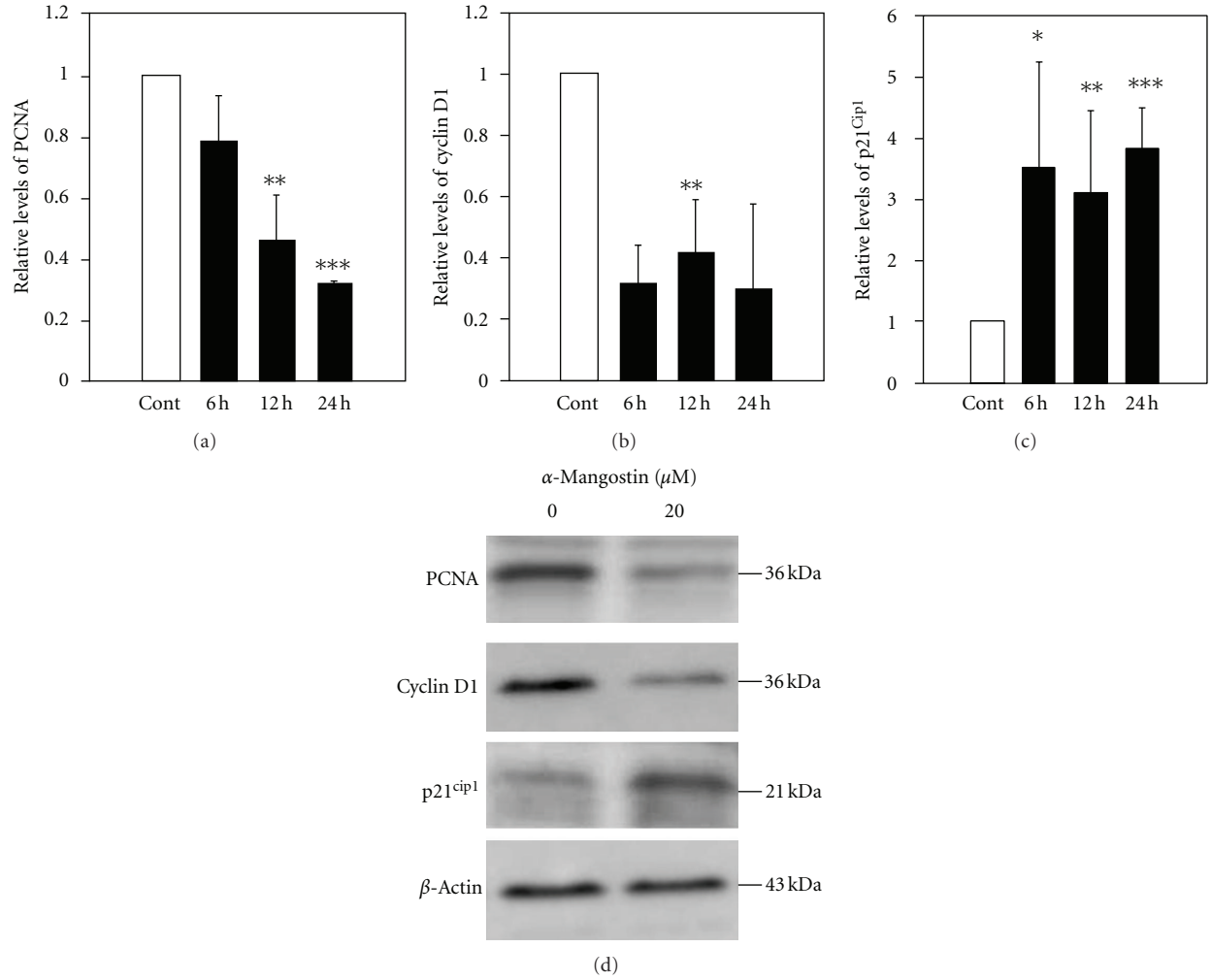

Figure 5: Changes in expression of genes involved in G1 phase regulation. (a)–(c) mRNA expressions of cell-cycle regulators for G1 phase, PCNA (a), cyclin D1 (b), and $p21^{cip1}$ (c), were examined using real-time PCR assays in MDA-MB231 cells after treatment with α-mangostin, as compared to controls. White bars indicate the results for controls and black bars indicate the results of analysis at 6 h, 12 h, and 24 h after treatment with α-mangostin ($^*P < 0.05$, $^{**}P < 0.01$). PCNA and cyclin D1 expressions were significantly lower and $p21^{cip1}$ was significantly higher in cells treated with α-mangostin for 24 h, as compared to controls. Relative target gene levels were calculated using the $\Delta\Delta$CT method. GAPDH was used as a reference gene. Data are presented as means ± SD of triplicate independent measurements. (d) Western blots of PCNA (36 kDa) and cyclin D1 (36 kDa) showed significantly lower levels, and $p21^{cip1}$ (21 kDa) showed significantly higher levels in cells treated with α-mangostin for 24 h, as compared to controls (left lane). These results were similar to those for PCR analysis, as shown in (a)–(c). β-Actin served as an internal control (lowest panel). Three samples from control and α-mangostin-treated cells were used for measurement.

and Erk5 phosphorylation involving the mitogen-activated protein kinase (MAPK) signaling pathway [5]. PI3K/Akt and Erk signaling target Bcl-2-associated agonists of cell death (Bad), a member of the Bcl-2 family. Bcl-2 family members are known to be regulators of programmed cell death. Bad promotes apoptosis by displacing Bax, another Bcl-2 family member, from binding to Bcl-2 and Bcl-xL, causing cytochrome *c* release from mitochondria [15]. These data suggest that apoptotic cell death caused by α-mangostin treatment in human mammary carcinoma cells occurs via mitochondria-mediated apoptosis, followed by inhibition of PI3K/Akt signaling pathway, and may include Bad activation.

3.4. Cell-Cycle Distribution. As measured by flow cytometry, 24 h exposure to 20 μM α-mangostin induced a significant elevation in the number of cells in the G1-phase, as compared with control cells (Figure 3(d)). There was also a significant reduction in the S-phase population in α-mangostin-treated cells (Figure 3(d)). These results suggest that G1-phase arrest was the result of α-mangostin inhibiting entry into S-phase.

3.5. Expression of Cell-Cycle Regulatory Genes. As α-mangostin treatment induced cell-cycle arrest, we investigated the expression of cell-cycle regulatory genes. Real-time analysis revealed that the expression of $p21^{cip1}$ was up-regulated and CHEK2 expression tended to increase for more than 6 h after α-mangostin treatment (Figure 4). $p21^{cip1}$ is a cyclin-dependent kinase inhibitor and the encoded protein binds to and inhibits the activity of cyclin-CDK2 (CDK: cyclin-dependent kinase) or -CDK4 complexes, thereby functioning

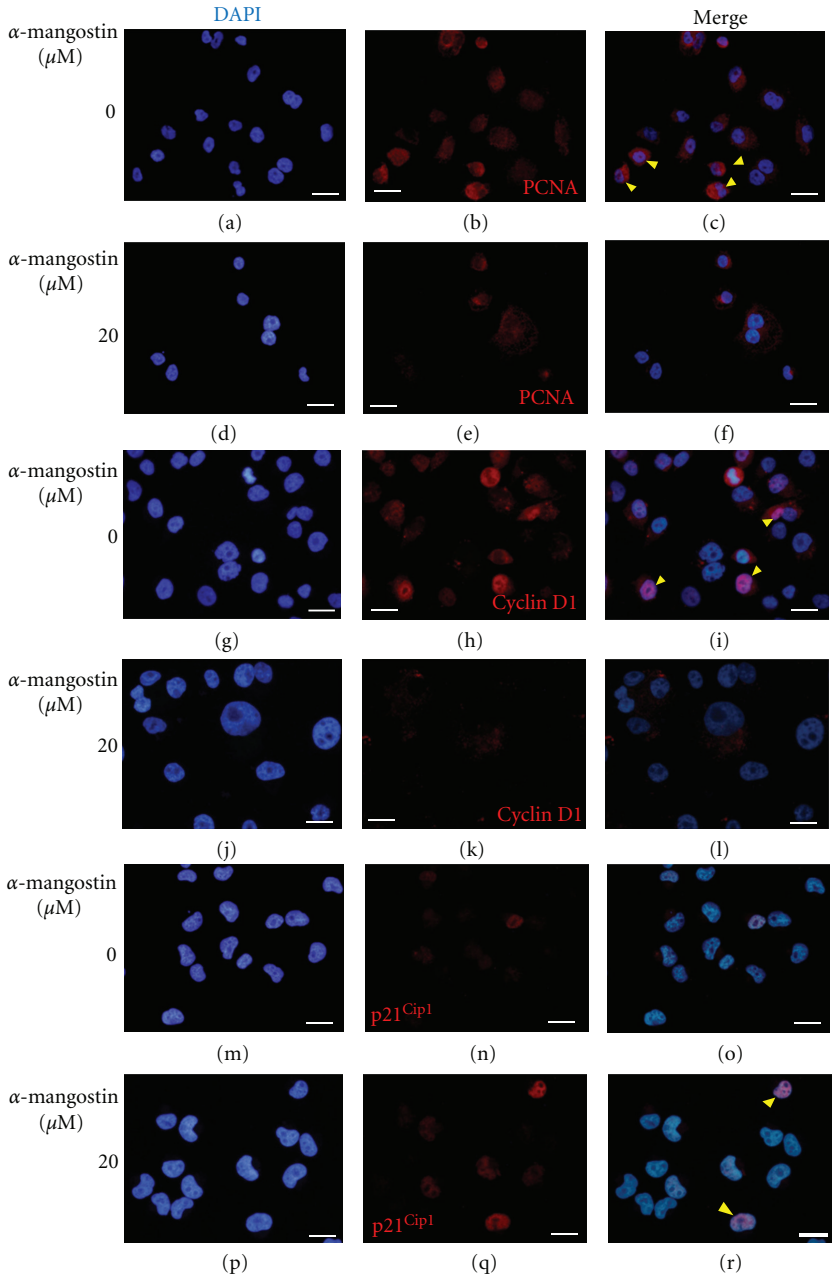

Figure 6: Expression of PCNA, cyclin D1 and $p21^{cip1}$ proteins after α-mangostin treatment. Immunofluorescence of PCNA (a)–(f), cyclin D1 (g)–(l), and $p21^{cip1}$ (m)–(r) in MDA-MB231 cells after 24 h of treatment with α-mangostin ((d)–(f), (j)–(l), (p)–(r)), as compared with controls ((a)–(c), (g)–(i), (m)–(o)). Yellow arrowheads in panels (c), (i), and (r) indicate higher expression of each protein in nuclei. PCNA and cyclin D1 expression was reduced and $p21^{cip1}$ expression were elevated in α-mangostin-treated cells, as compared to controls. Scale bars = 25 μm.

as a regulator of cell-cycle progression at the G1-phase [16]. CHEK2 is one of the cell-cycle checkpoint regulators and putative tumor suppressors that lead to G1-phase arrest through CDK phosphatase and cell division cycle 25 homolog A (cdc25A) phosphorylation [17]. Increases in $p21^{cip1}$ and CHEK2 expression lead to decreases in CDKs and cyclins, and G1-phase arrest and inhibition of cell proliferation, followed by decreases in proliferating cell nuclear antigen (PCNA). Furthermore, we confirmed the expression of G1/S-phase-related molecules, particularly $p21^{cip1}$, PCNA, and cyclin D1 by using Western blotting and immunofluorescence staining (Figures 5 and 6). On Western blotting analysis, PCNA (36 kDa) and cyclin D1 (36 kDa) protein were significantly lower, and $p21^{cip1}$ (21 kDa) protein was significantly elevated in cells treated with α-mangostin for 24 h, as compared to controls (Figure 5(d)). These results agreed with those of the real-time PCR analysis shown in Figures 4 and 5(a)–5(c). Immunofluorescence staining

revealed that PCNA and cyclin D1 expression were lower and that $p21^{cip1}$ expression was elevated in the nuclei of α-mangostin-treated cells, as compared to controls (Figure 6). These results suggest that α-mangostin induces G1-phase arrest and S-phase suppression by altering the expression of cell-cycle-related molecules, such as $p21^{cip1}$, CHEK2, cyclins, cdc(s), CDKs, and PCNA.

4. Conclusion

In conclusion, our results demonstrated that the therapeutic effects of α-mangostin are mediated by mitochondria-mediated apoptosis under control of the PI3K/Akt signaling pathway. α-Mangostin may be useful as a therapeutic agent for breast cancer carrying a p53 mutation and including HER2/hormone-negative subtypes.

Acknowledgments

This investigation involved Industry-Academic-Government collaboration as follows: PM Riken-yakka Ltd., Field & Device Co., Osaka Health Science University, Osaka Medical Collage, Gifu Pharmaceutical University, and a Grant-in-Aid for Private Universities from the Ministry of Education, Culture, Sports, Science and Technology of Japan. The authors thank Mr. Teruo Ueno (the Central Research Laboratory of Osaka Medical Collage) for assistance with the cell-cycle analysis.

References

[1] J. Baselga, D. Tripathy, J. Mendelsohn et al., "Phase II study of weekly intravenous trastuzumab (Herceptin) in patients with HER2/neu-overexpressing metastatic breast cancer," *Seminars in Oncology*, vol. 26, no. 4, supplement 12, pp. 78–83, 1999.

[2] H. Wildiers, C. Fontaine, P. Vuylsteke et al., "Multicenter phase II randomized trial evaluating antiangiogenic therapy with sunitinib as consolidation after objective response to taxane chemotherapy in women with HER2-negative metastatic breast cancer," *Breast Cancer Research and Treatment*, vol. 123, no. 2, pp. 463–469, 2010.

[3] N. S. Azad, E. M. Posadas, V. E. Kwitkowski et al., "Combination targeted therapy with sorafenib and bevacizumab results in enhanced toxicity and antitumor activity," *Journal of Clinical Oncology*, vol. 26, no. 22, pp. 3709–3714, 2008.

[4] K. R. Bauer, M. Brown, R. D. Cress, C. A. Parise, and V. Caggiano, "Descriptive analysis of estrogen receptor (ER)-negative, progesterone receptor (PR)-negative, and HER2-negative invasive breast cancer, the so-called triple-negative phenotype: a population-based study from the California Cancer Registry," *Cancer*, vol. 109, no. 9, pp. 1721–1728, 2007.

[5] Y. Akao, Y. Nakagawa, M. Iinuma, and Y. Nozawa, "Anti-cancer effects of xanthones from pericarps of mangosteen," *International Journal of Molecular Sciences*, vol. 9, no. 3, pp. 355–370, 2008.

[6] K. Matsumoto, Y. Akao, H. Yi et al., "Preferential target is mitochondria in α-mangostin-induced apoptosis in human leukemia HL60 cells," *Bioorganic and Medicinal Chemistry*, vol. 12, no. 22, pp. 5799–5806, 2004.

[7] P. Moongkarndi, N. Kosem, S. Kaslungka, O. Luanratana, N. Pongpan, and N. Neungton, "Antiproliferation, antioxidation and induction of apoptosis by Garcinia mangostana (mangosteen) on SKBR3 human breast cancer cell line," *Journal of Ethnopharmacology*, vol. 90, no. 1, pp. 161–166, 2004.

[8] K. Matsumoto, Y. Akao, K. Ohguchi et al., "Xanthones induce cell-cycle arrest and apoptosis in human colon cancer DLD-1 cells," *Bioorganic and Medicinal Chemistry*, vol. 13, no. 21, pp. 6064–6069, 2005.

[9] H. Doi, M. A. Shibata, E. Shibata et al., "Panaxanthone isolated from pericarp of Garcinia mangostana L. suppresses tumor growth and metastasis of a mouse model of mammary cancer," *Anticancer Research*, vol. 29, no. 7, pp. 2485–2495, 2009.

[10] M. A. Shibata, M. Iinuma, J. Morimoto et al., "α-Mangostin extracted from the pericarp of the mangosteen (Garcinia mangostana Linn) reduces tumor growth and lymph node metastasis in an immunocompetent xenograft model of metastatic mammary cancer carrying a p53 mutation," *BMC Medicine*, vol. 9, article 69, 2011.

[11] M. A. Shibata, Y. Miwa, J. Morimoto, and Y. Otsuki, "Easy stable transfection of a human cancer cell line by electrogene transfer with an Epstein-Barr virus-based plasmid vector," *Medical Molecular Morphology*, vol. 40, no. 2, pp. 103–107, 2007.

[12] J. Bartek, R. Iggo, J. Gannon, and D. P. Lane, "Genetic and immunochemical analysis of mutant p53 in human breast cancer cell lines," *Oncogene*, vol. 5, no. 6, pp. 893–899, 1990.

[13] P. M. O'Connor, J. Jackman, I. Bae et al., "Characterization of the p53 tumor suppressor pathway in cell lines of the National Cancer Institute anticancer drug screen and correlations with the growth-inhibitory potency of 123 anticancer agents," *Cancer Research*, vol. 57, no. 19, pp. 4285–4300, 1997.

[14] Y. Liang, J. Wu, G. M. Stancel, and S. M. Hyder, "P53-dependent inhibition of progestin-induced VEGF expression in human breast cancer cells," *Journal of Steroid Biochemistry and Molecular Biology*, vol. 93, no. 2–5, pp. 173–182, 2005.

[15] E. Yang, J. Zha, J. Jockel, L. H. Boise, C. B. Thompson, and S. J. Korsmeyer, "Bad, a heterodimeric partner for Bcl-x(L), and Bcl-2, displaces Bax and promotes cell death," *Cell*, vol. 80, no. 2, pp. 285–291, 1995.

[16] Y. Xiong, G. J. Hannon, H. Zhang, D. Casso, R. Kobayashi, and D. Beach, "p21 is a universal inhibitor of cyclin kinases," *Nature*, vol. 366, no. 6456, pp. 701–704, 1993.

[17] J. Falck, N. Mailand, R. G. Syljuåsen, J. Bartek, and J. Lukas, "The ATM-Chk2-Cdc25A checkpoint pathway guards against radioresistant DNA synthesis," *Nature*, vol. 410, no. 6830, pp. 842–847, 2001.